GDP-Perosamine Synthase: Structural Analysis and Production of a Novel Trideoxysugar[†,‡]

Paul D. Cook and Hazel M. Holden*

Department of Biochemistry, University of Wisconsin, Madison, Wisconsin 53706

Received December 12, 2007; Revised Manuscript Received January 10, 2008

ABSTRACT: Perosamine or 4-amino-4,6-dideoxy-D-mannose is an unusual sugar found in the *O*-antigens of some Gram-negative bacteria such as *Vibrio cholerae* O1 (the causative agent of cholera) or *Escherichia coli* O157:H7 (the leading cause of food-borne illnesses). It and similar deoxysugars are added to the *O*-antigens of bacteria via the action of glycosyltransferases that employ nucleotide-linked sugars as their substrates. The focus of this report is GDP-perosamine synthase, a PLP-dependent enzyme that catalyzes the last step in the formation of GDP-perosamine, namely, the amination of the sugar C-4′. Here we describe the three-dimensional structure of the enzyme from *Caulobacter crescentus* determined to a nominal resolution of 1.8 Å and refined to an *R*-factor of 17.9%. The overall fold of the enzyme places it into the well-characterized aspartate aminotransferase superfamily. Each subunit of the dimeric enzyme contains a seven-stranded mixed β-sheet, a two-stranded antiparallel β-sheet, and 12 α-helices. Amino acid residues from both subunits form the active sites of the GDP-perosamine synthase dimer. Recently, the structure of another PLP-dependent enzyme, GDP-4-keto-6-deoxy-D-mannose-3-dehydratase (or ColD), was determined in our laboratory, and this enzyme employs the same substrate as GDP-perosamine synthase. Unlike GDP-perosamine synthase, however, ColD functions as a dehydratase that removes the sugar C-3′ hydroxyl group. By purifying the ColD product and reacting it with purified GDP-perosamine synthase, we have produced a novel GDP-linked sugar, GDP-4-amino-3,4,6-trideoxy-D-mannose. Details describing the X-ray structural investigation of GDP-perosamine synthase and the enzymatic synthesis of GDP-4-amino-3,4,6-trideoxy-D-mannose are presented.

Perosamine[1] (4-amino-4,6-dideoxy-D-mannose) is an unusual dideoxysugar found in the *O*-antigen of *Vibrio cholerae* O1, the causative agent of cholera in humans (*1*). An *N*-acetylated version of it has also been isolated from a variety of Gram-negative bacteria, including *Escherichia coli* O157:H7, the infamous contaminant of packaged spinach that caused widespread infections in the United States in 2006 (*2*). The differences in the carbohydrate moieties forming the *O*-antigens of Gram-negative bacteria contribute to the amazing diversity of bacterial strains observed throughout nature. Many of the sugars isolated from the *O*-antigens are quite unusual and include tyvelose, perosamine, and colitose, among others. In addition to the bacterial *O*-antigens, perosamine is also found, for example, in the antibiotic perimycin synthesized by the Gram-positive bacterium *Streptomyces coelicolor* var. *aminophilus* (*3*).

As shown in Scheme 1, the biosynthetic pathway of GDP-perosamine begins with the formation of mannose 6-phosphate from fructose 6-phosphate (*4*). A bifunctional enzyme termed phosphomannose isomerase-guanosine diphosphomannose pyrophosphorylase or RfbA catalyzes this reaction. In the next step of the pathway, RfbB, a phosphomannomutase, converts mannose 6-phosphate to mannose 1-phosphate. Like most of the biosynthetic pathways for the production of unusual deoxysugars, the next reaction involves the attachment of mannose 1-phosphate (or more generally a hexose 1-phosphate) to a nucleotide monophosphate via the action of RfbA (Scheme 1). For perosamine synthesis, the nucleotide substrate is GTP. Subsequently, the sugar C-6′ hydroxyl group is removed, and the C-4′ hydroxyl group is oxidized to a keto functionality via the action of GDP-mannose 4,6-dehydratase. In the final step, the 4-keto group of GDP-4-keto-6-deoxymannose is aminated by the action of GDP-perosamine synthase. Note that GDP-4-keto-6-deoxymannose is also an intermediate in the pathway for colitose biosynthesis (Scheme 1).

The topic of this investigation is GDP-perosamine synthase cloned from *Caulobacter crescentus* CB15, a Gram-negative bacterium widely distributed in soil and aquatic environments (*5*). This organism has served as a model system for the study of cell cycle regulation and differentiation. On the basis of amino acid sequence analysis, the GDP-perosamine synthase

[†] This research was supported by NIH Grant DK47814 to H.M.H.

[‡] X-ray coordinates have been deposited in the Research Collaboratory for Structural Bioinformatics, Rutgers University, New Brunswick, N. J. (Protein Data Bank entry 3BN1).

* To whom correspondence should be addressed. E-mail: Hazel_Holden@biochem.wisc.edu. Fax: (608) 262-1319. Phone: (608) 262-4988.

[1] Abbreviations: ESI, electrospray ionization; HEPES, *N*-(2-hydroxyethyl)piperazine-*N*′-2-ethanesulfonic acid; HPLC, high-performance liquid chromatography; IPTG, isopropyl β-D-1-thiogalactopyranoside; MES, 2-(*N*-morpholino)ethanesulfonic acid; Ni-NTA, nickel-nitrilotriacetic acid; NMR, nuclear magnetic resonance; PCR, polymerase chain reaction; perosamine, 4-amino-4,6-dideoxy-D-mannose; PLP, pyridoxal 5′-phosphate; TEV, tobacco etch virus; Tris-HCl, 2-amino-2-(hydroxymethyl)-1,3-propanediol.

10.1021/bi702430d CCC: $40.75
Published on Web 02/05/2008

Scheme 1

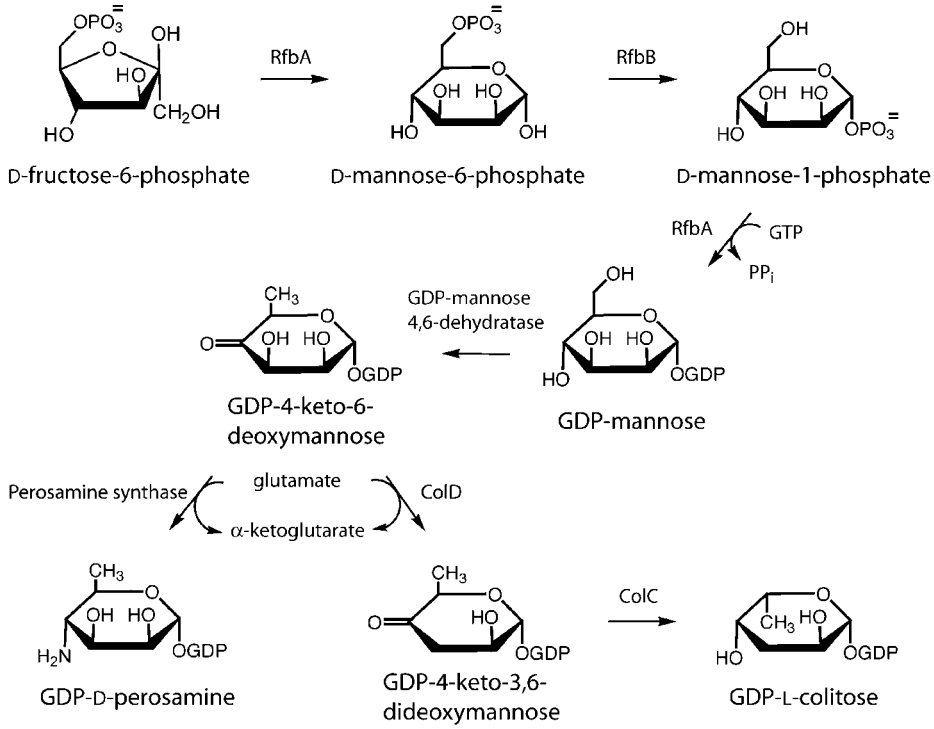

from *C. crescentus* is known to belong to the well-characterized aspartate aminotransferase superfamily (*6*). Members of this superfamily employ pyridoxal 5′-phosphate (PLP) as a cofactor which is typically held in the active site via a Schiff base with a conserved lysine residue. Biochemical studies on the GDP-perosamine synthases from both *V. cholerae* O1 and *E. coli* O157:H7 suggest differences in their quaternary structures, namely, tetramer and decamer, respectively (*7, 8*). The amino acid sequence of the *C. crescentus* enzyme used in this investigation is 41 and 45% identical to those of the GDP-perosamine synthases from *V. cholerae* O1 and *E. coli* O157:H7, respectively. Presumably, the reaction mechanisms for all three enzymes follow ping-pong kinetics whereby in the first transamination step L-glutamate binds in the active site, ultimately leading to the formation of PMP and α-ketoglutarate. Upon release of α-ketoglutarate, GDP-4-keto-6-deoxymannose binds to the active site, resulting in its conversion to the C-4′-amino derivative and regeneration of PLP (Scheme 1). The identities of the active site residues intimately involved in catalysis for the above-mentioned GDP-perosamine synthases are presently unknown, but it can be postulated that the conserved lysine residues play a key role.

Research interest in the biosynthetic pathways leading to the formation of unusual di- and trideoxysugars has intensified within recent years in part because of the need for generating new antibacterial agents. Many of the proteins involved in these pathways are targets for antimicrobial therapeutics. Furthermore, by understanding the structure and function of the enzymes in these pathways, it may be able to produce "designer" carbohydrates with varying substituents. Here we report a high-resolution structural analysis of GDP-perosamine synthase from *C. crescentus* complexed with PLP and α-ketoglutarate. In addition, we demonstrate that GDP-perosamine synthase can utilize GDP-4-keto-3,6-dideoxymannose as an alternate substrate, and indeed, we have enzymatically synthesized a novel 3-deoxy form of GDP-perosamine, namely GDP-4-amino-3,4,6-trideoxy-D-mannose.

EXPERIMENTAL PROCEDURES

Cloning of the GDP-Perosamine Synthase Gene (Per). The gene encoding GDP-perosamine synthase was PCR-amplified from *C. crescentus* genomic DNA (ATCC) using standard procedures. Subsequently, the purified PCR product was A-tailed and ligated into the pGEM-T vector (Promega) for screening and sequencing. A pGEM-T-*Per* vector construct of the correct sequence was then appropriately digested and ligated into the pET28JT vector (*9*). DH5-α *E. coli* cells were transformed with the resulting plasmid and plated onto LB agar plates supplemented with kanamycin. Multiple colonies were tested for the presence of the *Per* gene.

Protein Expression and Purification. The pET28JT-*Per* plasmid was used to transform HMS 174 *E. coli* cells (Novagen). The culture was grown in LB medium supplemented with kanamycin at 37 °C and subjected to shaking until an optical density of 0.75 was reached at 600 nm. The flasks were then cooled to room temperature and induced with 1 mM IPTG. Cells were subsequently allowed to express at 21 °C for 24 h following induction.

The cells were harvested by centrifugation and disrupted by sonication on ice. The lysate was cleared by centrifugation, and GDP-perosamine synthase was purified utilizing Ni-NTA resin (Qiagen) according to the manufacturer's instructions. Half of this purified preparation was incubated in the presence of 1 mM DTT and TEV protease in a 50:1 (GDP-perosamine synthase:TEV protease) molar ratio at room temperature for 36 h to remove the nickel affinity histidine tag. The TEV protease was subsequently removed via nickel column chromatography. The GDP-perosamine synthase preparations (both His-tagged and TEV-cleaved)

were dialyzed against 25 mM Tris-HCl (pH 8.0) and 100 mM NaCl. The preparations were concentrated to 30 mg/mL on the basis of an extinction coefficient of 1.40 M^{-1} cm^{-1}.

Crystallization of GDP-Perosamine Synthase. Crystallization conditions were first surveyed by the hanging drop method of vapor diffusion utilizing a sparse matrix screen developed in the laboratory. Large single crystals of the His-tagged form of GDP-perosamine synthase were subsequently grown via batch methods by mixing 20 μL of the protein solution (at 30 mg/mL) with 20 μL of a precipitant solution. The precipitant solution contained 100 mM MES (pH 6.5), 20% poly(ethylene glycol) 8000, 2 mM PLP, and 2 mM α-ketoglutarate. The crystals grew to maximum dimensions of ~0.1 mm × 0.3 mm × 0.6 mm in 2 weeks. They belonged to space group $P2_1$ with two dimers in the asymmetric unit and the following unit cell dimensions: $a = 50.3$ Å, $b = 152.9$ Å, $c = 105.7$ Å, $\beta = 102.1°$.

Structural Analysis of GDP-Perosamine Synthase. X-ray data to 1.8 Å resolution were collected with a Bruker Platinum 135 CCD detector system. The X-ray source was Cu Kα radiation from a Bruker Microstar H generator operated at 45 kV and 60 mA (courtesy of Bruker AXS, Madison, WI). Single crystals were transferred in three steps to a cryoprotectant solution containing 100 mM MES (pH 6.5), 100 mM NaCl, 24% poly(ethylene glycol) 8000, 15% ethylene glycol, 2 mM PLP, and 2 mM α-ketoglutarate. A single crystal was then frozen in a cryostream, and an X-ray data set was collected. These data were processed with SAINT [Bruker (2003) *SAINT*, version V7.06A, Bruker AXS Inc., Madison, WI] and internally scaled with SADABS [Sheldrick, G. M. (2002) *SADABS*, version 2005/1, Bruker AXS Inc., Madison, WI]. Relevant X-ray data collection statistics are presented in Table 1.

The structure of GDP-perosamine synthase was determined via molecular replacement with Phaser (*10, 11*), employing ArnB, a 4-amino-4-deoxy-L-arabinose lipopolysaccharide-modifying enzyme (*12*) as the search model (PDB entry 1MDO, amino acid sequence identity of 34%). All solvent molecules and the coordinates for the PLP cofactors were omitted from the search probe. An initial solution produced a model with a starting *R*-factor of 41% to 1.8 Å resolution. Electron densities corresponding to the four subunits in the asymmetric unit were subsequently averaged with DM (*13*), and an "averaged" model was manually built with Coot (*14*). The model was then placed into the four positions in the asymmetric unit and subjected to least-squares refinement with TNT (*15*). Alternate cycles of manual model rebuilding and least-squares refinement resulted in an overall model *R*-factor of 17.9% for all measured X-ray data from 30 to 1.8 Å. Relevant refinement statistics are given in Table 1.

Gel Permeation Assay. The molar mass of the native TEV-cleaved GDP-perosamine synthase was estimated by size exclusion chromatography using an ÄKTA Purifier HPLC system (Amersham-Pharmacia Biotech) equipped with a Superdex 200 gel filtration column (Amersham Biosciences). The mobile phase was 50 mM Tris-HCl (pH 8.0) and 100 mM NaCl. The flow rate was 0.75 mL/min, and the column was calibrated using gel chromatography standards (Sigma) according to the manufacturer's instructions. The TEV-cleaved GDP-perosamine synthase eluted with an apparent native molar mass of 79 kDa.

Table 1: X-ray Data Collection and Least-Squares Refinement Statistics

space group	$P2_1$
unit cell dimensions	$a = 50.3$ Å, $b = 152.9$ Å, $c = 105.7$ Å, $\beta = 102.1°$
resolution limits (Å)	30–1.8
no. of independent reflections	141987 (20715)[a]
completeness	98.5 (96.1)[a]
redundancy	8.5 (3.6)[a]
avg I/avg $\sigma(I)$	16.9 (3.4)[a]
R_{sym}[b] (%)	8.1 (36.0)[a]
R-factor[c] (overall) (%)/no. of reflections	17.9/141981
R-factor (working) (%)/no. of reflections	17.6/127806
R-factor (free) (%)/no. of reflections	25.3/14175
no. of protein atoms[d]	1232
no. of heteroatoms[e]	693
weighted root-mean-square deviations from ideality	
bond lengths (Å)	0.013
bond angles (deg)	1.9
trigonal planes (Å)	0.009
general planes (Å)	0.018
torsional angles[f] (deg)	17.0
average B values	
protein atoms[g] (Å^2)	21.9
ligands (Å^2)	32.2
solvent (Å^2)	26.6

[a] Statistics for the highest-resolution bin from 1.9 to 1.8 Å. [b] $R_{sym} = (\sum|I - \bar{I}|/\sum I) \times 100$. [c] R-factor $= (\sum|F_o - F_c|/\sum|F_o|) \times 100$, where F_o is the observed structure factor amplitude and F_c is the calculated structure factor amplitude. [d] These include multiple conformations for Thr 29 in subunit 1, Val 162 and Ile 225 in subunit 2, Lys 43 and Ile 188 in subunit 3, and Met 287 in subunit 4. [e] Heteroatoms include 1209 waters, one sodium ion, one α-ketoglutarate, and three acetates. [f] The torsional angles were not restrained during the refinement. [g] The average B-factor for the protein atoms includes the PLP cofactors.

Production of GDP-Perosamine. The GDP-mannose-4,6-dehydratase required for the production of GDP-perosamine was prepared as previously described (*16*). GDP-perosamine was produced by reacting 5 mM GDP-mannose (Sigma), 20 mM L-glutamate, 1 mM PLP, 1 mM $NADP^+$, 3 μM GDP-mannose-4,6-dehydratase, and 3 μM GDP-perosamine synthase in buffer A [50 mM HEPES (pH 7.5) and 50 mM NaCl]. The reaction mixture was incubated at room temperature for 4 h, after which it was passed through a 30 kDa cutoff filter (Amicon) to remove the protein.

Contaminants were removed from the reaction flow-through using an ÄKTA Purifier HPLC system (Amersham-Pharmacia Biotech) equipped with a Resource-Q 6 mL anion exchange column (Amersham Biosciences). The column was first equilibrated with buffer B [20 mM ammonium bicarbonate (pH 8.5)], after which the reaction flow-through was loaded onto the column, washed, and eluted with a linear gradient to 60% buffer C [500 mM ammonium bicarbonate (pH 8.5)]. The flow rate was 6 mL/min, and the elution was monitored at 253 nm. The fractions containing GDP-perosamine were pooled and freeze-dried with a Labconco 1 L Freezone lyophilizer. The identity of the GDP-perosamine product was confirmed by ESI mass spectrometry (Mass Spectrometry/Proteomics Facility at the University of Wisconsin) and NMR spectroscopy (Nuclear Magnetic Resonance Facility, University of Wisconsin): ESI mass spectrometry parent ion at m/z 587.2; ^{1}H NMR (400 MHz, D_2O) δ 7.99 (1H, s, H-1 base), 5.82 (1H, d, H-1 ribose, $J =$ 6.1 Hz), 5.38 (1H, dd, H-1′ hexose, $J = 1.5$ Hz, $J = 7.5$ Hz), 4.67 (1H, H-2 ribose, under the water peak), 4.39 (1H,

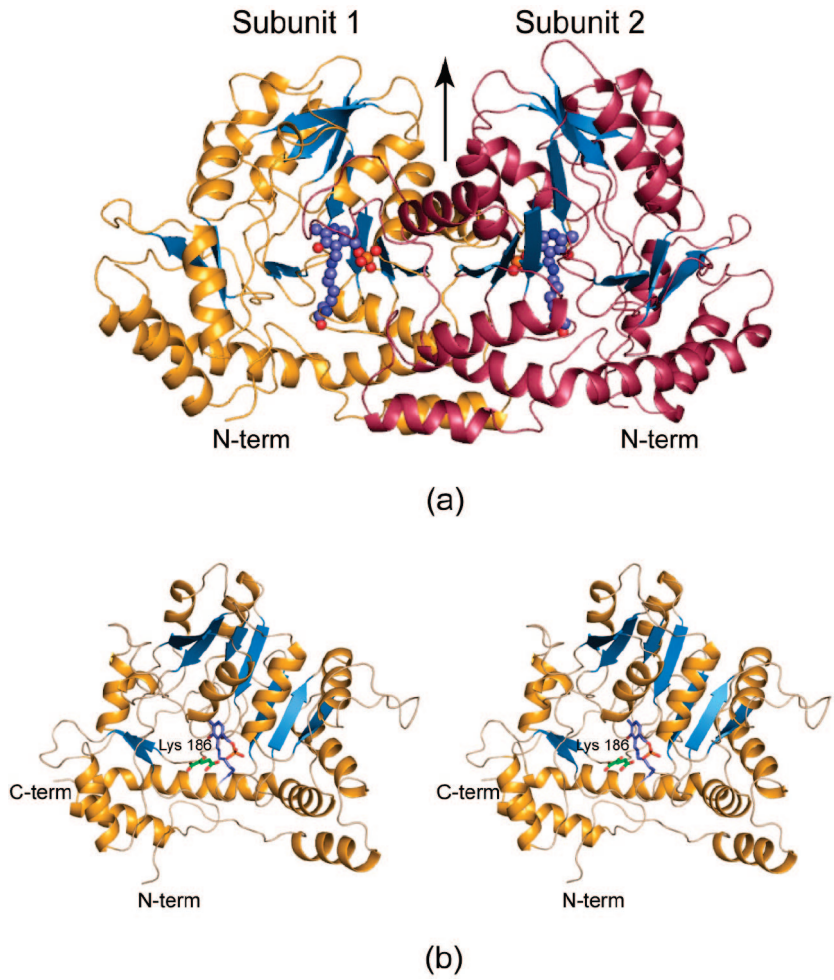

FIGURE 1: Structure of *C. crescentus* GDP-perosamine synthase. (a) A ribbon representation of the GDP-perosamine synthase dimer. Subunits 1 and 2 are colored gold and red, respectively, with the β-strands highlighted in blue. In each subunit, there is a Schiff base between Lys 186 and PLP, as indicated by the spheres. The dyad relating the two subunits lies in the plane of the page and is indicated by the arrow. (b) Stereo representation of subunit 1. Lys 186, the PLP cofactor, and α-ketoglutarate are displayed in stick representation. This figure and Figures 2 and 3 were generated with PyMOL (*29*).

m, H-3 ribose), 4.24 (1H, dd, H-5′ hexose), 4.10−4.06 (3H, including H-5 ribose and H-4 ribose), 3.97 and 3.93 (2H, including H-3′ and H-2′ hexose), 3.05 (1H, t, H-4′ hexose, J = 10.4 Hz), 1.22 (3H, d, H-6′ hexose, J = 6.2 Hz).

Production of GDP-4-Keto-3,6-dideoxy-D-mannose. GDP-4-keto-3,6-dideoxymannose was produced and purified in the same manner as GDP-perosamine, but GDP-4-keto-6-deoxy-mannose-3-dehydratase (ColD) was substituted for GDP-perosamine synthase. The product identity was confirmed by ESI mass spectrometry and NMR spectroscopy: ESI mass spectrometry parent ion at *m/z* 570.2; ^{1}H NMR (400 MHz, D_2O) δ 7.99 (1H, s, H-1 base), 5.82 (1H, d, H-1 ribose, J = 6.0 Hz), 5.39 (1H, d, H-1′ hexose, J = 7.3 Hz), 4.68 (H-2 ribose, under the water peak), 4.51 (1H, q, H-5′ hexose, J = 6.6 Hz), 4.40 and 4.23 (3H, m, including H-3 ribose and H-4 ribose), 4.10 (3H, m, including H-5 ribose), 2.91 (1H, dd, H-3′$_{eq}$ hexose, J = 3.9 Hz, J = 16.0 Hz), 2.32 (1H, dd, H-3′$_{ax}$ hexose, J = 2.9 Hz, J = 15.9 Hz), 1.10 (3H, d, H-6′ hexose, J = 6.6 Hz).

Production of GDP-4-Amino-3,4,6-trideoxy-D-mannose. A mixture containing 4 mM GDP-4-keto-3,6-dideoxymannose, 50 mM L-glutamate, 0.1 mM PLP, and 10 μM GDP-perosamine synthase in buffer A was incubated at room temperature for 8 h. The reaction mixture was passed through a 30 kDa cutoff filter and was purified by HPLC using a Resource-Q 6 mL anion exchange column. The column was equilibrated with buffer D [25 mM HEPES (pH 7.5)], after which the reaction flow-through was loaded onto the column, washed, and eluted with a linear gradient to 35% buffer E [25 mM HEPES (pH 7.5) and 1 M NaCl]. A new peak was observed in addition to GDP-4-keto-3,6-dideoxymannose. Fractions corresponding to this new peak were pooled, desalted, and lyophilized. The contents of this peak were characterized by ESI mass spectrometry and NMR spectroscopy: ESI mass spectrometry parent ion at *m/z* 571.3; ^{1}H NMR (400 MHz, D_2O) δ 8.12 (1H, s, H-1 base), 5.92 (1H, d, H-1 ribose, J = 6.2 Hz), 5.34 (1H, d, H-1′ hexose, J = 7.2 Hz), 4.78 (1H, H-2 ribose, under the water peak), 4.51 (1H, dd, H-3 ribose, J = 3.5 Hz), 4.35 (1H, m, H-3 ribose), 4.20 (2H, dd, H-5 ribose, J = 4.6), 4.12 and 3.98 (2H, m, including H-2′ hexose), 3.19 (1H, m, H-4′ hexose), 2.05 (2H, m, H-3′$_{ax}$ and H-3′$_{eq}$ hexose), 1.26 (3H, d, H-6′ hexose, J = 6.2 Hz).

RESULTS AND DISCUSSION

Overall Structure of GDP-Perosamine Synthase. The crystals used in this investigation contained four polypeptide chains in the asymmetric unit. On the basis of both gel filtration chromatography and visual inspection of the

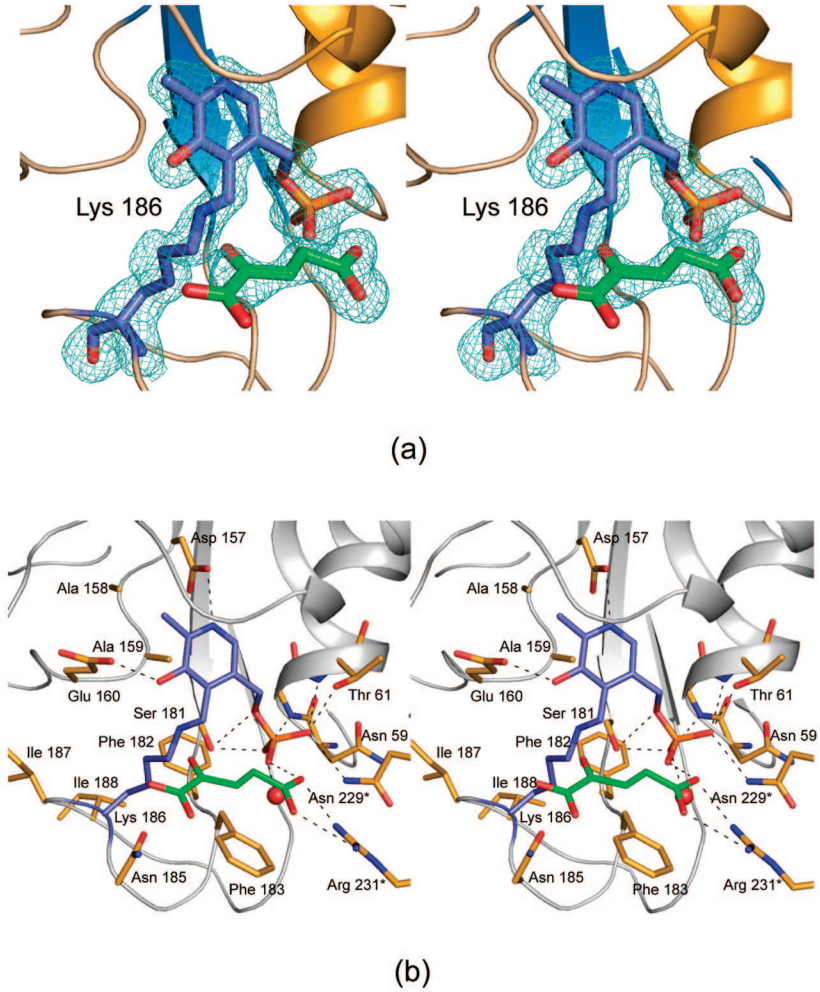

FIGURE 2: Active site of *C. crescentus* GDP-perosamine synthase. (a) Electron density corresponding to the Schiff base between Lys 186 and the PLP cofactor (highlighted in slate) and the α-ketoglutarate moiety (colored green). The map was calculated with coefficients of the form ($F_o - F_c$), where F_o was the native structure factor amplitude and F_c was the calculated structure factor amplitude. Atoms corresponding to Lys 186, the PLP cofactor, and α-ketoglutarate were excluded from the coordinate file during the least-squares refinement. The map was contoured at 3σ. (b) Stereoview of the active site. Those residues lying within ~3.5 Å of the PLP cofactor are highlighted with gold bonds. Lys 186 and the PLP cofactor are depicted with slate bonds, whereas the α-ketoglutarate is depicted with green bonds. Amino acid residues marked by an asterisk belong to subunit 2 of the dimer. Possible hydrogen bonds (within 3.2 Å) are indicated by the dashed lines.

contents of the asymmetric unit, it can be concluded that the *C. crescentus* GDP-perosamine synthase is dimeric with each subunit containing 371 amino acid residues. The model geometries for both dimers in the asymmetric unit are good with a total of 88, 12, and 0.1% of the amino acid residues lying in the core, allowed, and generously allowed regions of the Ramachandran plot, respectively. Overall, the electron densities corresponding to the four polypeptide chains in the asymmetric unit were reasonably well ordered except for the first few residues at the N-terminus of each subunit. Given that the electron density corresponding to the first dimer in the X-ray coordinate file was slightly better, the following discussion refers to it.

A ribbon representation of the GDP-perosamine synthase dimer, with overall dimensions of ~63 Å × 85 Å × 60 Å, is presented in Figure 1a. The two subunits interact extensively with a total buried surface area of 4500 Å^2, and their respective active sites are separated by ~25 Å. There are two regions that provide extensive subunit−subunit interactions. One of these regions is delineated by Arg 19−Ser 33, which contains the first α-helix of the subunit and a loop connecting it to the second α-helix. The second region is defined by Tyr 221−Gln 236 which folds into a random coil arrangement. Both of these regions from one subunit project toward the active site of the second subunit (and vice versa). A stereoview of subunit 1 of the dimer is displayed in Figure 1b. Its fold is dominated by a seven-stranded mixed β-sheet flanked on either side by three α-helices. There are six additional α-helices and a two-stranded antiparallel β-sheet that serve to complete the three-dimensional architecture of the subunit.

The crystals of GDP-perosamine synthase were grown in the presence of α-ketoglutarate. Shown in Figure 2a are the electron densities corresponding to both the internal aldimine (Lys 186 and PLP in a Schiff base) and an α-ketoglutarate molecule in subunit 1. As can be seen, the electron density for the internal aldimine is well-ordered as is the γ-carboxylate group of α-ketoglutarate. The rest of the α-ketoglutarate moiety is less ordered, and indeed, in the other subunits in the asymmetric unit, only an "acetyl" group could be positioned into the electron density. The structure presented here corresponds to an abortive complex, but presumably, the position of the α-ketoglutarate moiety shown in Figure 2a mimics that for the true substrate, L-glutamate.

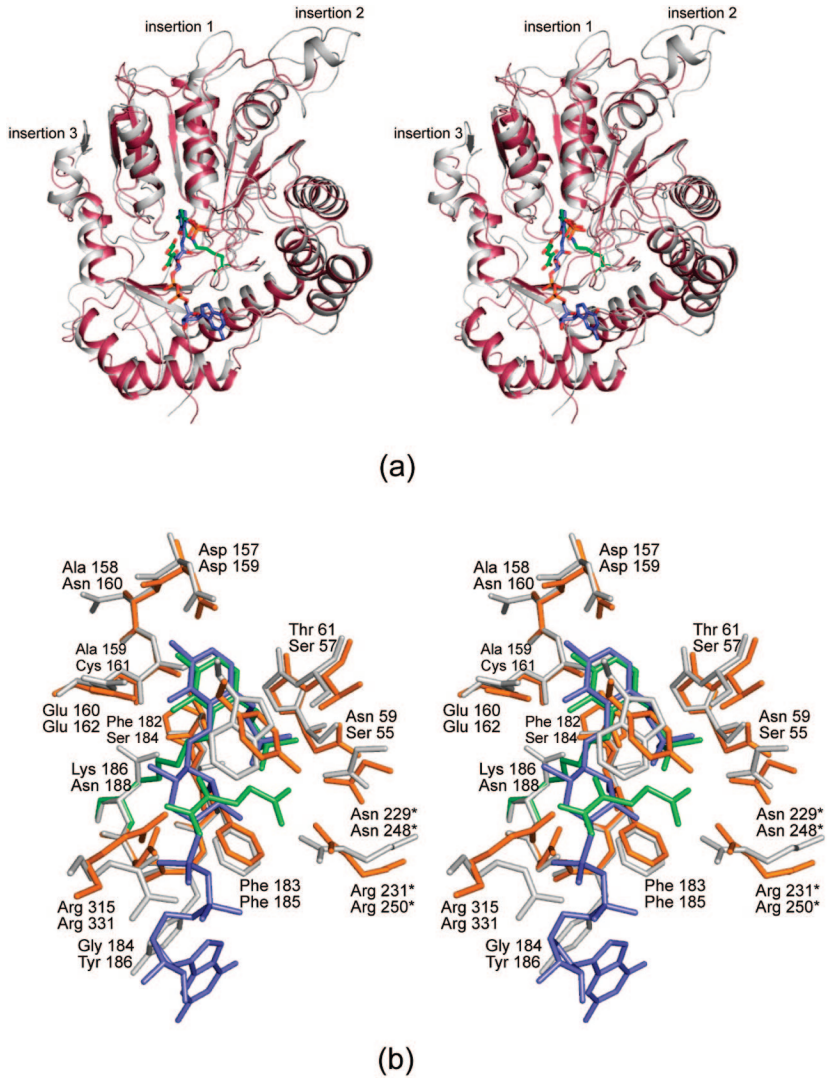

FIGURE 3: Comparison of GDP-perosamine synthase with ColD. (a) Superposition of the GDP-perosamine synthase and ColD models. GDP-perosamine synthase and ColD are colored red and white, respectively. There are three major insertions in ColD versus GDP-perosamine synthase as indicated. (b) Close-up view of the GDP-perosamine synthase and ColD active sites. GDP-perosamine synthase and ColD are highlighted with gold and white bonds, respectively. The internal aldimine in GDP-perosamine synthase is colored green, whereas the external aldimine formed between PLP and GDP-perosamine in ColD is colored slate. For clarity, Tyr 86 and Asn 185 in GDP-perosamine synthase and Trp 88 and Ser 187 in ColD are not labeled.

A close-up view of the active site for subunit 1 is depicted in Figure 2b. The pyridoxal ring of the cofactor is anchored to the protein via two hydrogen bonds. One of these occurs between the ring C-3 hydroxyl group and the side chain carboxylate of Glu 160, whereas the second is formed between the ring nitrogen and the carboxylate group of Asp 157. The phosphoryl moiety of the cofactor forms hydrogen bonds with the side chains of Thr 61, Ser 181, and Asn 229 (contributed by subunit 2). Additional interactions occur between the phosphoryl oxygens of the cofactor and the backbone amide groups of Gly 60 and Thr 61. There is one ordered water molecule located within 3.2 Å of the PLP moiety. The α-ketoglutarate is positioned such that its side chain carboxylate forms a salt bridge with the guanidinium group of Arg 231 from subunit 2. Interestingly, one of the carboxylate oxygens of α-ketoglutarate lies within 2.4 Å of a PLP phosphoryl oxygen, suggesting that this phosphoryl oxygen is protonated (Figure 2b).

Our interest in GDP-perosamine synthase arose from recent structural work in the laboratory on GDP-4-keto-6-deoxy-D-mannose-3-dehydratase, hereafter referred to as ColD (*16–18*). This enzyme catalyzes the third step in the production of colitose, a 3,6-dideoxysugar found in the *O*-antigens of some Gram-negative bacteria (*19–21*) and marine bacteria (*22, 23*). As indicated in Scheme 1, ColD uses the same substrate as GDP-perosamine synthase but instead removes the C-3′ hydroxyl group from the sugar rather than aminating the C-4′ position. Both ColD and GDP-perosamine synthase are dimeric PLP-dependent enzymes, but in the case of the former, the cofactor is not covalently attached to the protein by a Schiff base with a lysine residue. Instead, the lysine is replaced with a histidine, and the cofactor is never covalently bound to the enzyme. ColD and GDP-perosamine synthase share 23% amino acid sequence identity, and their α-carbon traces correspond with a root-mean-square deviation of 1.4 Å for 330 structurally equivalent atoms. Shown in Figure 3a is a superposition of their overall subunit folds. There are three major insertions in ColD relative to GDP-perosamine synthase. The first is a six-residue insertion after Leu 67 (ColD). The second is a rather large 17-residue insertion after Asn 220, which results in an additional α-helical turn in ColD. Finally, there is an

insertion in ColD after Thr 342, which results in an additional α-helix and a β-strand as shown in Figure 3a.

A close-up view of the active sites for GDP-perosamine synthase and ColD is presented in Figure 3b. The structure of ColD shown is that of a site-directed mutant protein in which the active site histidine residue has been replaced with an asparagine. In addition, its structure was determined in the presence GDP-perosamine which reacted with PLP to form an external aldimine. As can be seen in Figure 3b, the α-ketoglutarate moiety observed in GDP-perosamine synthase lies in a position similar to that occupied by the hexose moiety in ColD, and the PLP cofactors adopt similar positions in both enzymes. The similarities between the ColD and GDP-perosamine synthase active sites extend beyond the PLP and sugar/α-ketoglutarate ligands. Indeed, the active sites are remarkably similar with perhaps the only notable exceptions being the replacements of Ser 184, Tyr 186, and Ser 187 in ColD with a phenylalanine, a glycine, and a asparagine, respectively, in GDP-perosamine synthase. Given that the aromatic side chain of Tyr 186 in ColD forms an important stacking interaction with the guanine ring of the nucleotide-linked sugar, it is possible that in GDP-perosamine synthase the nucleotide and phosphoryl moieties of the substrate are anchored to the enzyme in a somewhat different manner. Experiments designed to address this issue are presently underway.

Enzymatic Activity Assays. As discussed above, GDP-perosamine synthase catalyzes the PLP-dependent amination of the C-4′ keto group of GDP-4-keto-6-deoxymannose (Scheme 1). The catalytic activity of the *C. crescentus* GDP-perosamine synthase employed for the X-ray crystallographic studies described here was confirmed by incubating the enzyme in the presence of GDP-mannose, GDP-mannose 4,6-dehydratase, $NADP^+$, PLP, and L-glutamate. Samples of this reaction mixture taken over time and subjected to HPLC showed the appearance of a new peak (data not shown), which was confirmed to be GDP-perosamine by ESI mass spectrometry and ^1H NMR analyses.

The similarities between GDP-perosamine synthase and ColD in both their cofactor requirements and substrate specificities led us to question whether the ColD reaction product, GDP-4-keto-3,6-dideoxymannose, could function as a substrate for GDP-perosamine synthase. To test this hypothesis, the ColD product, GDP-4-keto-3,6-dideoxymannose (Scheme 1), was first synthesized and purified. An HPLC trace of this pure compound is shown in Figure 4A. Note that the ColD product has a retention time of 6.6 min. In the next experiment, GDP-perosamine synthase was incubated in the presence of the ColD product, PLP, and excess L-glutamate. An HPLC trace of this reaction is shown in Figure 4B. In addition to the peak at 6.6 min, a new peak with a retention time of 3.5 min appeared. Both ESI mass spectrometry data and ^1H NMR analyses of this new peak are consistent with GDP-4-amino-3,4,6-trideoxy-D-mannose, which we will call GDP-3-deoxyperosamine. A search of the literature suggests that GDP-3-deoxyperosamine has not been observed in nature thus far.

Given their similar active site architectures, one compelling question is why ColD functions as a dehydratase whereas GDP-perosamine synthase catalyzes a simple amino transfer. A perusal of their respective active sites shows their striking similarity with the exception of the active site lysine in GDP-perosamine being replaced with a histidine in ColD. It has been suggested that this histidine residue in ColD functions as the active site base required for catalysis (*17, 24*). Most likely, Lys 186 in GDP-perosamine synthase also serves as an active site base. However, whether a particular enzyme functions as a dehydratase or an aminotransferase probably results from a combination of subtle factors, including the manner in which the sugar-linked nucleotide is bound in the active site and perhaps the type of sugar conformation assumed by the hexose moiety. In ColD, for example, the perosamine group adopts the less commonly observed $B_{2,5}$ rather than the more typical $^4C_1$ conformation (*18*).

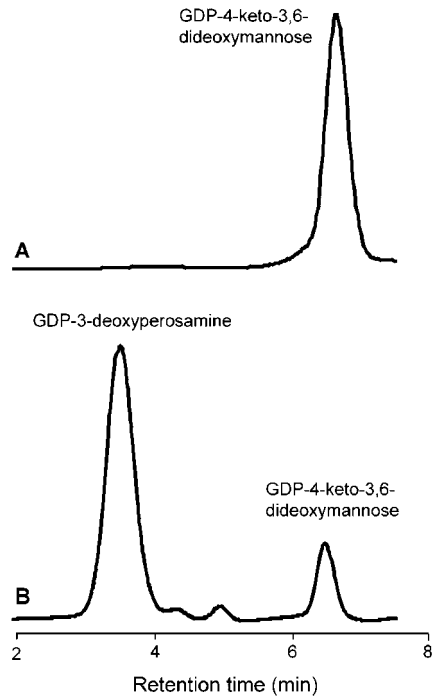

FIGURE 4: Production of GDP-3-deoxyperosamine. The HPLC elution profile for the pure ColD product (GDP-4-keto-3,6-dideoxymannose) with a retention time of 6.6 min is shown in panel A. The HPLC elution profile when GDP-perosamine synthase is incubated with the ColD product, PLP, and excess L-glutamate is shown in panel B. The new peak appears at 3.5 min and corresponds to GDP-3-deoxyperosamine.

A second major question is why GDP-perosamine synthase demonstrates substrate promiscuity by accepting a 3-deoxy version of its natural substrate. This question is more easily addressed. The structure of ColD complexed with a nucleotide-linked sugar shows that the hydroxyl groups on C-2′ and C-3′ form hydrogen bonds with ordered water molecules rather than protein side chains. Furthermore, the C-3′ hydroxyl group of the sugar points toward Phe 185 which is conserved as Phe 183 in GDP-perosamine synthase. One can speculate that GDP-perosamine synthase also coordinates the sugar hydroxyls via water molecules, and thus, removal of the C-3′ hydroxyl group would still allow the substrate to bind in a catalytically competent manner.

In summary, by understanding the structure of GDP-perosamine synthase and its relationship to ColD, we have been able to produce a unique nucleotide-linked sugar, GDP-3-deoxyperosamine. This result has important ramifications given that many macrolide antibiotics are biologically inactive or less potent without the appropriate sugar moieties appended to their aglycone lactone rings (*25, 26*). It has been

shown that removal of one or more hydroxyl group(s) from the sugar scaffold results in molecules with completely different physiochemical and pharmacokinetic properties. The use of nucleotide-linked deoxysugars as tools for altering the glycosylation patterns of macrolide rings represents a powerful approach for the design of new therapeutics (*27, 28*). Clearly, antibiotics, such as the β-lactams and the macrolides, have dramatically changed the course of human existence as is evidenced by the increased life expectancy following the introduction of penicillin to the general population in the 1940s. Unfortunately, as is so often the case with the use of antibiotics, bacteria become resistant over a period of time. The attachment of 3-deoxyperosamine or other novel sugars to macrolide scaffolds has the potential of producing new therapeutics, which may prove to be important in management strategies against bacterial resistance.

ACKNOWLEDGMENT

We gratefully acknowledge the helpful discussions of Drs. James B. Thoden and W. W. Cleland. We also thank Dr. Mathew M. Benning (Bruker AXS Inc.) for help with X-ray data collection.

REFERENCES

1. Redmond, J. W. (1975) 4-Amino-4,6-dideoxy-D-mannose (D-perosamine): A component of the lipopolysaccharide of *Vibrio cholerae* 569B (Inaba). *FEBS Lett. 50*, 147–149.
2. Wang, L., and Reeves, P. R. (1998) Organization of *Escherichia coli* O157 *O* antigen gene cluster and identification of its specific genes. *Infect. Immun. 66*, 3545–3551.
3. Lee, C. H., and Schaffner, C. P. (1966) Perimycin: Chemistry of perosamine. *Tetrahedron Lett. 47*, 5837–5840.
4. Stroeher, U. H., Karageorgos, L. E., Brown, M. H., Morona, R., and Manning, P. A. (1995) A putative pathway for perosamine biosynthesis is the first function encoded within the rfb region of *Vibrio cholerae* O1. *Gene 166*, 33–42.
5. Poindexter, J. S. (1981) The *caulobacters*: Ubiquitous unusual bacteria. *Microbiol. Rev. 45*, 123–179.
6. Jansonius, J. N. (1998) Structure, evolution and action of vitamin B_6-dependent enzymes. *Curr. Opin. Struct. Biol. 8*, 759–769.
7. Albermann, C., and Piepersberg, W. (2001) Expression and identification of the RfbE protein from *Vibrio cholerae* O1 and its use for the enzymatic synthesis of GDP-D-perosamine. *Glycobiology 11*, 655–661.
8. Zhao, G., Liu, J., Liu, X., Chen, M., Zhang, H., and Wang, P. G. (2007) Cloning and characterization of GDP-perosamine synthetase (Per) from *Escherichia coli* O157:H7 and synthesis of GDP-perosamine *in vitro*. *Biochem. Biophys. Res. Commun. 363*, 525–530.
9. Thoden, J. B., Timson, D. J., Reece, R. J., and Holden, H. M. (2005) Molecular structure of human galactokinase: Implications for Type II galactosemia. *J. Biol. Chem. 280*, 9662–9670.
10. Storoni, L. C., McCoy, A. J., and Read, R. J. (2004) Likelihood-enhanced fast rotation functions. *Acta Crystallogr. D60*, 432–438.
11. Read, R. J. (2001) Pushing the boundaries of molecular replacement with maximum likelihood. *Acta Crystallogr. D57*, 1373–1382.
12. Noland, B. W., Newman, J. M., Hendle, J., Badger, J., Christopher, J. A., Tresser, J., Buchanan, M. D., Wright, T. A., Rutter, M. E., Sanderson, W. E., Muller-Dieckmann, H. J., Gajiwala, K. S., and Buchanan, S. G. (2002) Structural studies of *Salmonella typhimurium* ArnB (PmrH) aminotransferase: A 4-amino-4-deoxy-L-arabinose lipopolysaccharide-modifying enzyme. *Structure 10*, 1569–1580.
13. Cowtan, K., and Main, P. (1998) Miscellaneous algorithms for density modification. *Acta Crystallogr. D54*, 487–493.
14. Emsley, P., and Cowtan, K. (2004) Coot: Model-building tools for molecular graphics. *Acta Crystallogr. D60*, 2126–2132.
15. Tronrud, D. E., Ten Eyck, L. F., and Matthews, B. W. (1987) An efficient general-purpose least-squares refinement program for macromolecular structures. *Acta Crystallogr. A43*, 489–501.
16. Cook, P. D., and Holden, H. M. (2007) A structural study of GDP-4-keto-6-deoxy-D-mannose-3-dehydratase: Caught in the act of *geminal* diamine formation. *Biochemistry 46*, 14215–14224.
17. Cook, P. D., Thoden, J. B., and Holden, H. M. (2006) The structure of GDP-4-keto-6-deoxy-D-mannose-3-dehydratase: A unique coenzyme B6-dependent enzyme. *Protein Sci. 15*, 2093–2106.
18. Cook, P. D., and Holden, H. M. (2007) GDP-4-Keto-6-deoxy-D-mannose-3-dehydratase: Accommodating a sugar substrate in the active site. *J. Biol. Chem.* (in press).
19. Edstrom, R. D., and Heath, E. C. (1965) Isolation of colitose-containing oligosaccharides from the cell wall lipopolysaccharide of *Escherichia coli*. *Biochem. Biophys. Res. Commun. 21*, 638–643.
20. Kotandrova, N. A., Gorshkova, R. P., Zubkov, V. A., and Ovodov Iu, S. (1989) The structure of the *O*-specific polysaccharide chain of the lipopolysaccharide of *Yersinia pseudotuberculosis* serovar VII. *Bioorg. Khim. 15*, 104–110.
21. Xiang, S. H., Haase, A. M., and Reeves, P. R. (1993) Variation of the rfb gene clusters in *Salmonella enterica*. *J. Bacteriol. 175*, 4877–4884.
22. Muldoon, J., Perepelov, A. V., Shashkov, A. S., Gorshkova, R. P., Nazarenko, E. L., Zubkov, V. A., Ivanova, E. P., Knirel, Y. A., and Savage, A. V. (2001) Structure of a colitose-containing *O*-specific polysaccharide of the marine bacterium *Pseudoalteromonas tetraodonis* IAM 14160(T). *Carbohydr. Res. 333*, 41–46.
23. Silipo, A., Molinaro, A., Nazarenko, E. L., Gorshkova, R. P., Ivanova, E. P., Lanzetta, R., and Parrilli, M. (2005) The *O*-chain structure from the LPS of marine halophilic bacterium *Pseudoalteromonas carrageenovora*-type strain IAM 12662T. *Carbohydr. Res. 340*, 2693–2697.
24. Alam, J., Beyer, N., and Liu, H. W. (2004) Biosynthesis of colitose: Expression, purification, and mechanistic characterization of GDP-4-keto-6-deoxy-D-mannose-3-dehydrase (ColD) and GDP-L-colitose synthase (ColC). *Biochemistry 43*, 16450–16460.
25. Weymouth-Wilson, A. C. (1997) The role of carbohydrates in biologically active natural products. *Nat. Prod. Rep. 14*, 99–110.
26. Harms, J. M., Bartels, H., Schlunzen, F., and Yonath, A. (2003) Antibiotics acting on the translational machinery. *J. Cell Sci. 116*, 1391–1393.
27. Rupprath, C., Schumacher, T., and Elling, L. (2005) Nucleotide deoxysugars: Essential tools for the glycosylation engineering of novel bioactive compounds. *Curr. Med. Chem. 12*, 1637–1675.
28. Thibodeaux, C. J., Melancon, C. E., and Liu, H. W. (2007) Unusual sugar biosynthesis and natural product glycodiversification. *Nature 446*, 1008–1016.
29. DeLano, W. L. (2002) The PyMOL Molecular Graphics System, DeLano Scientific LLC, San Carlos, CA.

BI702430D